

Distinguishing Quark and Gluon Partons in the the Pion and Kaon

Kyle D. Bednar,¹ Ian C. Cloët,² and Peter C. Tandy^{1,3}

¹Center for Nuclear Research, Department of Physics, Kent State University, Kent OH 44242 USA

²Physics Division, Argonne National Laboratory, Argonne, IL 60439 USA

³CSSM, Department of Physics, University of Adelaide, Adelaide SA 5005, Australia

(Dated: November 28, 2018)

The leading-twist parton distribution functions of the pion and kaon are calculated with the first full implementation of the Rainbow-Ladder truncation of QCD's Dyson-Schwinger equations. The gluonic dressing of the quarks is accounted for by the solution of the integral equation for the quark vertex relevant to the defining Deep-Inelastic Scattering process. At the model scale of 0.781 GeV, this approach immediately distinguishes 65% of the pion's light-cone momentum as due to quarks and the remaining 35% as due to the dressing gluons. For kaons, the momentum fractions are 70% and 30%. From scale evolution, these pion momentum fractions link easily with those found recently by analysis of experiment, along with calculations within lattice-regulated QCD. Separation of the gluon dressing tends to reshape the quark distribution by moving strength from low quark x to high x , but the $(1-x)^2$ endpoint exponent of low scale QCD is preserved in this approach.

Introduction: In contrast to the early simple models of baryons as three constituent quarks, and mesons as quark-antiquark states, recent progress in understanding the structure of hadrons is marked by revelations of the separate roles of quarks and gluons. A consensus is starting to emerge [1] from experimental and theoretical work on integral properties such as the quark and gluon parton contributions to the nucleon spin, angular momentum, and lightcone momentum [2, 3]. For the pion meson, the gluon and quark parton fractions of the lightcone momentum obtained from just a few data analyses [4] are in qualitative agreement. A more complete understanding requires experimental and theoretical extraction of the probability distribution of the various partons with longitudinal lightcone momentum fraction x correlated with transverse momentum or position. Standard lattice QCD techniques can achieve precision for just the first few moments of parton distributions [1]. Promising spacelike correlator and other methods to extend the reach are under development [5–8].

Gluons have a dynamical role as part of a dressed quark or via the mediation of interactions between two or more quarks and gluons. It is possible that one of these roles dominates the net gluon parton distribution, and even integrated quantities like the gluon fraction of the nucleon spin and momentum (roughly 50% [3] and 30% [4] respectively at scales 1-4 GeV). The parton x distributions of quarks and gluons are certainly correlated by the strong quark dressing in QCD.

To advance understanding in this area, we use a truncation of QCD which implements a self-consistent Ladder-Rainbow dressing of quarks to calculate the quark parton x distribution as distinguished from the dressing gluons. Since the latter emphasizes low x , the distinguished quark distribution will tend to be stronger at high x than otherwise. This is a mechanism that can possibly bridge the gap between the recent experimental analysis [4] that favored a high x fit $(1-x)^b$ with $b \approx 1$ and an earlier analysis [9] that favored $b \approx 2$. Complicating this topic is the fact that a variety of theoretical approaches [10–15] produce a derivative at the endpoint characterized by $b = 2$ at a low hadronic scale as driven

by the ultraviolet behavior of the 1-gluon exchange binding mechanism.

The DSE-RL description of hadron physics has proven to be very efficient for ground state masses, decay constants, and electromagnetic form factors [16–19]. It has been especially accurate for light quark pseudoscalar mesons because their properties are strongly dictated by the dynamical breaking of chiral symmetry, which is built into the approach. It has recently been applied to the nucleon spin-independent PDFs [20] within a previously advocated approximation that did not distinguish dressing quark partons from dressing gluons.

Rainbow-Ladder Truncation of QCD: A central element of this symmetry-preserving truncation [13–15, 21–23], is the gap equation for the dressed-quark propagator

$$S^{-1}(k) = Z_2 (i\not{k} + Z_m m_r) - \int_p^\Lambda \frac{\lambda^a}{2} \gamma_\mu \mathcal{K}_{\mu\nu}(p-k) S(p) \frac{\lambda^a}{2} \gamma_\nu, \quad (1)$$

where m_r is the renormalized current quark mass, and \int_p^Λ represents $\int \frac{d^4p}{(2\pi)^4}$ with Λ indicating the ultraviolet regularization mass scale. The general form of the solution is $S^{-1}(k) = i\not{k}A(k^2, \zeta^2) + B(k^2, \zeta^2)$, where ζ is the renormalization scale where $A \rightarrow 1$ and $B \rightarrow m_r$. The employed RL kernel $\mathcal{K}_{\mu\nu}$ is described later.

Meson Parton Distribution Functions: At leading order in the Bjorken hard-scattering limit, the PDF for meson M is given by the correlator [24–27] :

$$q_f(x) = \frac{1}{4\pi} \int d\lambda e^{-ixP \cdot n\lambda} \times \langle M(P) | \bar{\psi}_f(\lambda n) \not{n} W(\lambda, n \cdot A) \psi_f(0) | M(P) \rangle_c, \quad (2)$$

where $q_f(x)$ is the probability of quark parton with flavor f having light-cone longitudinal momentum $xP \cdot n$. In Minkowski metric the light-like longitudinal basis vector is given by $n^\mu = (1, \mathbf{0}_T, -1)$ in the target rest frame. The DSE

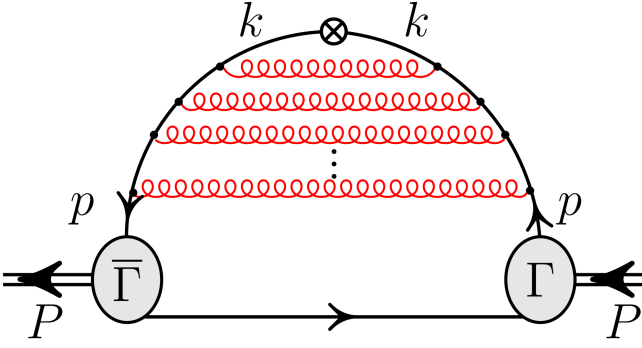


Figure 1. Illustration of the Rainbow-Ladder quark vertex for the DIS process. All quark propagators are dressed. k is the quark parton light-cone momentum, and Bjorken $x = k^+/P^+$. The constituent quark p can be treated as the parton only in the limit of zero momentum carried by dressing gluons.

approach is based on equations that couple n -point Green functions and does not easily accommodate the Wilson line $W(\lambda, n \cdot A)$ that enforces strict color gauge invariance in Eq. (2). In light-cone gauge ($n \cdot A = 0$), the Wilson line is formally unity [26]; however, the established elements of the DSE approach are available in Landau gauge. The challenge of a rigorous DSE-RL treatment of the Wilson line for PDFs is thus postponed; however, we note that the numerical impact on leading-twist PDFs has been estimated to be small – albeit in a very different approach [28].

In the RL truncation, the PDF moments $\int_0^1 dx x^m q_f(x)$ can be expressed as

$$\langle x^m \rangle_f = N_c \text{tr}_d \int_p^\Lambda \bar{\Gamma}_M(p_r, P) S(p) \Gamma_n^{(m)}(p) S(p) \times \Gamma_M(p_r, P) S(p - P), \quad (3)$$

where $\Gamma_M(p_r, P)$ is the Bethe-Salpeter bound state amplitude in RL truncation having the $q\bar{q}$ relative momentum $p_r = p - P/2$. The moments of the quark-parton PDF vertex in Eq. (3) are $\Gamma_n^{(m)}(p) = \int_0^1 dx x^m \Gamma_n(p, x)$ where the vector vertex $\Gamma_n(p, x) = n_\nu \Gamma_\nu(p, x)$ is defined by the Bethe-Salpeter integral equation [14]

$$\Gamma_n(p, x) = Z_2 i \not{n} \delta(p \cdot n - xP \cdot n) - \int_k^\Lambda \gamma_\mu \mathcal{K}_{\mu\nu}(p - k) S(k) \Gamma_n(k, x) S(k) \gamma_\nu. \quad (4)$$

Every quark propagator required at this level is non-perturbative and fully dressed by the same gap equation. The perturbative description of the struck quark within the initial handbag diagram of the forward Compton process has been accounted for by the hard Bjorken kinematic limit of the DIS probability that has produced the triangle diagram with the hard vertex contribution having net Dirac matrix \not{n} [24–26].

The physical picture is clarified by the first iteration or

1-loop contribution to $\Gamma_n(p, x)$:

$$- \int_k^\Lambda \gamma_\mu \mathcal{K}_{\mu\nu}(p - k) S(k) Z_2 i \not{n} S(k) \gamma_\nu \delta(k \cdot n - xP \cdot n). \quad (5)$$

The parton momentum specified by x is always that of the (dressed) quark that connects to the gamma matrix \not{n} in a diagrammatic sense, i.e., k and not p in Fig. 1. All succeeding iterations provide more gluon dressing that carry more of the dressed quark's momentum. The first DSE-RL implementation [14] of the meson PDF quark triangle diagram, as represented by Eq. (3), introduced an *Ansatz* for this vertex to greatly simplify the calculation so that other physics issues could be investigated. Since the DSE-RL kernel $\mathcal{K}_{\mu\nu}(p - k)$ has strongest support in the infrared where $k \approx p$, it was assumed [14] reasonable to treat the integral term of Eq. (4) by the substitution $\Gamma_n(k, x) \approx \delta(p \cdot n - xP \cdot n) \Gamma_n^{(0)}(p)$. This produces the *Ward-Identity Ansatz* for the quark PDF vertex

$$\Gamma_n(p, x) \approx \Gamma_{n\Lambda}(p, x) = \delta(p \cdot n - xP \cdot n) n^\mu \frac{\partial S^{-1}(p)}{\partial p^\mu}. \quad (6)$$

This approximates the quark parton momentum fraction x in terms of the quark momentum p offered by the hadron state rather than the true parton momentum k revealed after exchanged gluon are identified as part of the spectator system. See Fig. 1. It is exact for the 0^{th} moment of the vertex, thus conserving quark number or equivalently electromagnetic current. All higher moments will be overestimated. To date, this *Ward-Identity Ansatz* has been employed for all DSE-RL studies. Its inability to distinguish the x support of quarks from that of the dressing gluons is explored in this work.

Quark Parton Distribution Functions: To illustrate further the light-cone momentum fraction content of the dressed quark vertex, and how it bears upon that of the hadron x support, it is convenient to introduce z as the parton momentum fraction with respect to the momentum p of the dressed quark offered by the meson. That is, $z = k \cdot n / p \cdot n = xP \cdot n / p \cdot n = x/y$, where y is the fraction of meson momentum carried by the dressed quark it provides to the DIS process. Then vertex Eqs. (4) and (5) become equations for the purely quark amplitude $\Lambda_n(p, z)$ defined by $|p \cdot n| \Gamma_n(p, x) = \Lambda_n(p, z)$ and given by

$$\Lambda_n(p, z) = Z_2 i \not{n} \delta(z - 1) - \int_k^\Lambda \gamma_\mu \mathcal{K}_{\mu\nu}(p - k) S(k) \frac{|p \cdot n|}{|k \cdot n|} \Lambda_n(k, z \frac{p \cdot n}{k \cdot n}) S(k) \gamma_\nu. \quad (7)$$

Analysis of the 1-loop contribution from the first iteration, similar to Eq. (5), confirms that parton momentum fraction z is always that of the dressed quark that connects to the matrix \not{n} , internal to gluon dressings in a diagrammatic sense, and measured relative to the external quark momentum p .

The moments of the quark vertex $\Gamma_n(p, x)$ have the invariant form

$$\Gamma_n^{(m)}(p) = \frac{1}{|P \cdot n|} \left(\frac{p \cdot n}{P \cdot n} \right)^m \left(i \not{p} f_1^{(m)} + 2n \cdot p (i \not{p} f_2^{(m)} + f_3^{(m)}) \right) \quad (8)$$

where the $f_i^{(m)}(p^2) = \int_0^1 dz z^m f_i(p, z)$ are moments of intrinsic quark parton distributions associated with the 3 Dirac structures. The *Ward-Identity Ansatz* is equivalent to $f_i(p^2, z) \rightarrow \delta(z-1) \{A(p^2), A'(p^2), B'(p^2)\}$. The further limit of a contact interaction, or NJL model [29], would produce $f_i(p^2, z) \rightarrow \delta(z-1) \{1, 0, 0\}$.

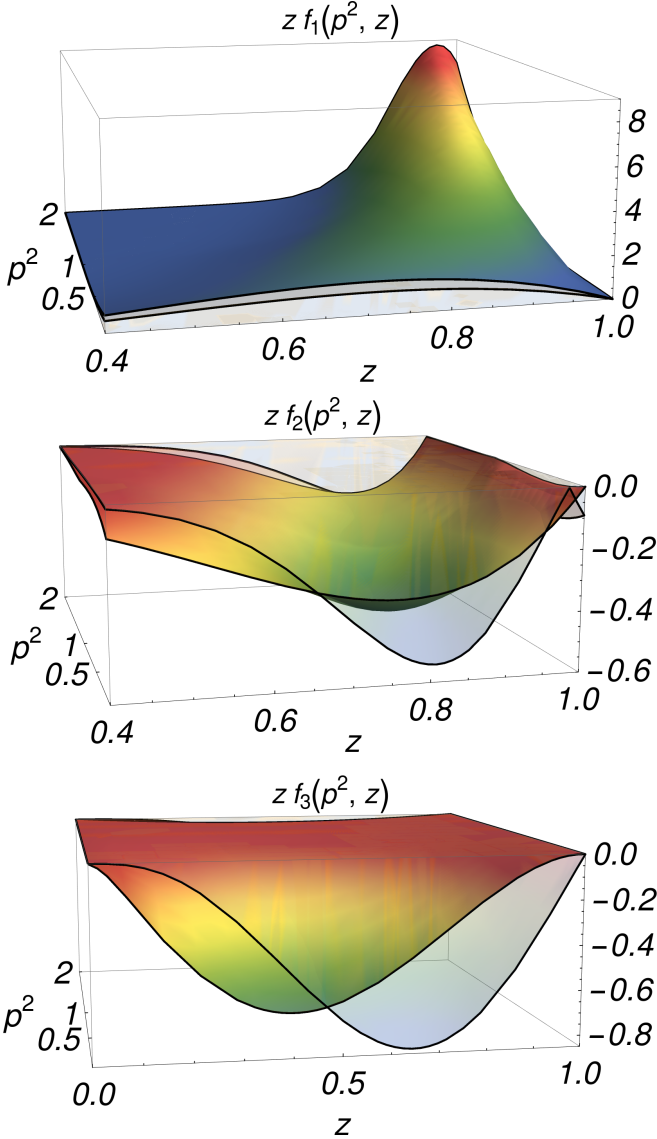


Figure 2. The vertex amplitudes $f_i(p^2, z)$ describing the dressed quark PDF. p is the dressed quark momentum and z is the momentum fraction of the interior quark parton. Color depicts degenerate u- and d-quarks; grey depicts the s-quark in the vertex relevant to the kaon.

PDF	Q (GeV)	$\langle x \rangle$	$\langle x^2 \rangle$	$\langle x^3 \rangle$	$\langle x^4 \rangle$
u^π DSE-RL	0.781	0.323	0.167	0.109	0.083
u^π WI-An	0.458	0.482	0.290	0.201	0.155
u^K DSE-RL	0.781	0.297	0.148	0.092	0.065
u^K WI-An	0.458	0.461	0.268	0.177	0.128
s^K DSE-RL	0.781	0.402	0.221	0.143	0.101
s^K WI-An	0.458	0.514	0.321	0.223	0.167
JAM [4]	1.3	0.268	0.127	0.074	0.048
u^π DSE-RL	1.3	0.268	0.125	0.076	0.054
u^π WI-An	1.3	0.268	0.114	0.059	0.037
ASV [9]	1.3	0.247	0.106	0.055	0.033
LQCD [33]	2.0	0.27	0.13	0.074	

Table I. DSE-RL results for low moments compared to the most recent experimental analysis JAM, the older ASV analysis, and unquenched lattice-QCD. The difference between $\langle x \rangle_\pi$ using the DSE-RL vertex and the *Ward-Identity Ansatz* illustrates that at least 30% of the dressed-quark's light-cone momentum is gluonic.

Quark Calculations and Analysis: In this work we employ a numerical implementation in Euclidean metric where the model for the RL kernel has been well-constrained in the form [30] $\mathcal{K}_{\mu\nu}(q) = Z_2^2 \mathbf{G}(q^2) D_{\mu\nu}^{free}(q)$ where $\mathbf{G}(q^2)$ is the effective running coupling whose ultraviolet form is 1-loop renormalized QCD and its infrared form is a 1-parameter representation of a large amount of hadron physics [16–19].

To illustrate some of the underlying dynamics, the quark parton distributions $f_i(p^2, z)$ are obtained from 9 moments $f_i^{(m)}(p^2)$ via a fit to the form $x^\alpha (1-x)^\beta (1+c\sqrt{x})$. The important qualitative feature evident in Fig. 2 is the distributed z support as distinct from the *Ward-Identity Ansatz* result $\delta(z-1)$. Since f_1 for $p < 1$ GeV is strongest at $z \sim 0.6-0.8$, it is not surprising that the first moment yields $f_1^{(1)}(p^2) \sim 0.65 A(p^2)$ at typical virtuality $p^2 \sim (0.2 \text{ GeV})^2$. All higher moments have slightly greater reduction factors compared to the *Ward-Identity Ansatz* result.

This reduction is a direct consequence of the finite momentum carried by the RL kernel $\mathcal{K}_{\mu\nu}(q)$ leaving less for the dressed quark partons. Our final meson $\langle x \rangle$ results reflect this. Effects of dynamical chiral symmetry breaking are evident in Fig. 2 by the differing gray surfaces which apply to the strange quark vertex; the heavier quark carries more momentum.

Meson Calculations and Analysis: The pseudoscalar meson solution for the Bethe-Salpeter bound state amplitude has the general form [31, 32]

$$\Gamma_M(k; P) = \gamma_5 [iE_M(k; P) + \gamma \cdot P F_M(k; P) + \gamma \cdot k G_M(k; P) - \sigma_{\mu\nu} k_\mu P_\nu H_M(k; P)], \quad (9)$$

where the $E_M(k; P)$, etc, are the invariant amplitudes. This is employed in numerical evaluation of Eq. (3) for the meson PDF moments. With $\langle x^0 \rangle_q = 1$, the next 4 moments are presented in Table I. The meson moments are fit to those of

$$q_V(x) = N_0 (x^{\alpha_1} (1-x)^2 (1+c_1\sqrt{x}) + c_2 x^2 + c_3 x^{\alpha_2} + c_4 x^{\alpha_3}) + N_1 (1-x)^3, \quad (10)$$

with the parameters provided in Table II. We impose an end-point exponent of 2 [10–15] and allow the possibility of significant strength at otherwise large x . The model scale is fixed so that $\langle x \rangle_q^\pi$ evolves via NLO DGLAP to the result 0.268 from the recent experimental analysis [4] at scale $Q = 1.3$ GeV. This yields pion model scales $Q_0 = 0.781$ GeV for the DSE-RL result and $Q_0 = 0.458$ GeV for the Ward-Identity *Ansatz* result.¹ Without independent information, the kaon model scale is taken to be the same in each case.

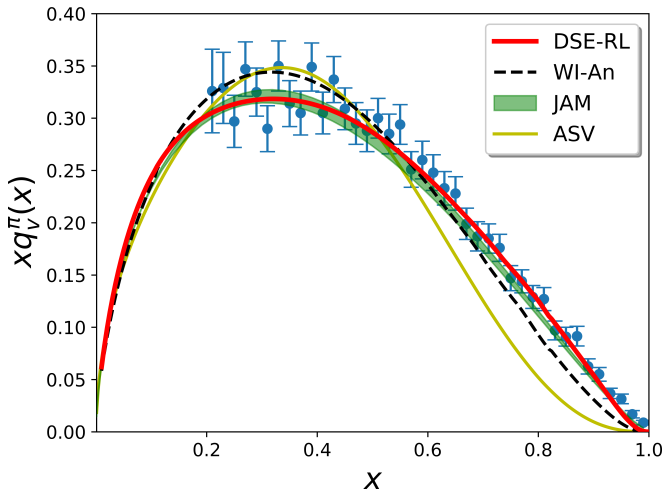


Figure 3. The pion’s valence-quark distribution at $Q = 5.2$ GeV compared to data [36]. The solid red curve represents the DSE-RL approach implemented fully here for the first time. The dashed curve is from the Ward-Identity *Ansatz* used in previous DSE-RL works. The green band is the recent JAM-JLab data analysis [4]; the yellow curve is the earlier NLO soft-gluon-resummation analysis [9]. All curves shown, except JAM, have end-point power behavior $(1-x)^2$, consistent with current theory.

The DSE-RL approach, at its model scale, explicitly contains two processes which permit gluons to carry a significant fraction of quark momentum. These are: gluon dressing of the quark PDF vertex and the self-energy in the quark propagators. Both are important in hadron physics, but the former very directly impacts the x support of quark PDFs of hadrons. Even a one-loop approximation to the quark vertex diminishes the quark parton momentum fraction by $\sim 30\%$, close to the full result.

The DSE-RL recognition of the intrinsic x support provided by the dressing glue cannot be totally offset by a change in model scale. Since the x support provided by glue is strongest at small x , one can also expect a shift in the net quark x distribution to stronger support at larger x . The only question is the strength in this shift. In Fig. 3 the pion DSE-RL PDF result at scale 5.2 GeV shows significantly stronger high- x support than the Ward-Identity *Ansatz* result at the same scale. Table I confirms that higher DSE-RL moments are larger at the same scale. We note that mechanisms capable of shifting

¹ Evolution is done at NLO using APFEL [34]; JAM grids are accessed with LHAPDF [35].

PDF	N_1	α_i	c_i
u^π DSE-RL	0.16	(2.82,6.69,26.07)	(0.08,-0.81,2.62,7.99)
u^π WI-An	0.0025	(0.93,10.82,38.28)	(-1.25,1.99,7.80,49.11)
u^K DSE-RL	0.20	(2.87,4.76,7.85)	(0.18,-0.90,0.14,2.74)

Table II. Parameters for fits to the moments at the model scale, $Q_0 = 0.781$ GeV for the DSE-RL vertex and $Q_0 = 0.458$ GeV for the Ward Identity *Ansatz*.

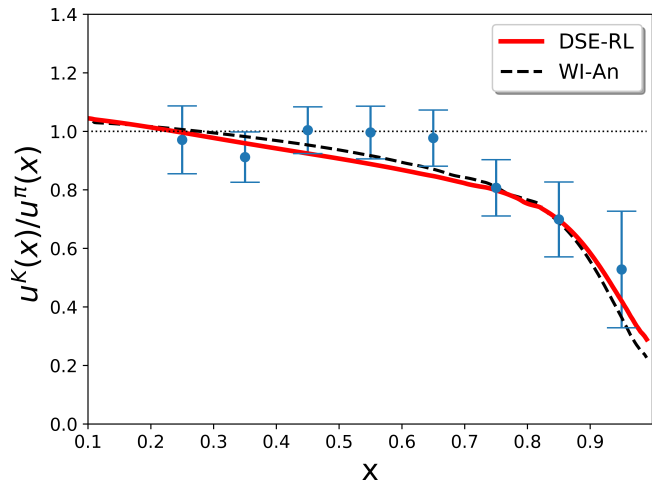


Figure 4. The ratio u^K/u^π compared to data [37].

momentum to sea quarks, such as meson cloud dressing [20], will raise the model scale for valence PDFs.

Table I shows that the DSE-RL description immediately gives the valence (dressed) quark $\langle x \rangle$ results: 65% for the pion and 70% for the kaon, at model scale. The remaining momentum in the present dynamical approach is that carried by the dressing gluons as illustrated in Fig. 1. In contrast, the Ward-Identity vertex *Ansatz* ignores the dressing substructure to produce $\langle x \rangle_\pi \rightarrow 0.96$, with the shortfall most likely due to this vertex not being representative of a true DIS mechanism compatible with Eq. (2).

Results in Table I demonstrate flavor symmetry breaking in the kaon. Heavier quarks force gluon dressing dynamics to take up a lesser momentum fraction and this is illustrated by the s- and u-quark contributions to the kaon PDFs in Table I. In the flavor symmetry limit, the pion results are $\langle x \rangle_u = \langle x \rangle_d = 0.323$. In the kaon, the average flavor shift is 16% with the DSE-RL vertex, and 5.5% using the WI *Ansatz* vertex. The former number is compatible with the estimate of 15% from the different peaks of the PDF distributions found in Ref. [14] and the well-defined asymmetry of the leading kaon Distribution Amplitude reported in Ref. [38]. The present estimate correlates well with the u and s quark dressed masses where $(M_s - M_u)/(M_s + M_u) = 7\%$ at $p^2 = 0$ or 11% for Euclidean constituent masses. The quark current mass asymmetry ($\sim 66\%$) is overshadowed by the masses added by dynamical chiral symmetry breaking. Fig. 4 displays the ratio u^K/u^π compared to data [37] to illustrate the environmental

effect. The different treatments of the vertex largely cancel in this ratio.

Summary and Outlook: In QCD, as in its DSE-RL truncation, the definition of the quark parton momentum fraction applies to the in- and out- dressed quark momentum relative to the Dirac matrix γ^+ that arises in the hard Bjorken limit. The quark momentum outside or prior to the infinite number of gluon exchange dressings of the hard DIS coupling has a different character of x support that does not distinguish quark and gluon contributions. The dressed DSE-RL vertex for the quark PDF automatically makes this distinction, and identifies 65% of the pion's light-cone momentum fraction as being carried by dressed quarks, in agreement with the recent experimental analysis [4] at a correspondingly low hadronic scales. The proportion is 70% for the kaon. The rest is gluons in the DSE-RL organization. This is immediately within 5-10% of experiment [4] without fine tuning for sea quark effects or scale evolution. The reshaping of the x distribution of the quark PDF that naturally follows is an important element. The obtained PDF description remains consistent with an endpoint exponent of 2 at low scale, but nevertheless produces strength at high x consistent with the recent experimental analysis. Our analysis suggests that a QCD model can produce a hard power fit $\sim (1-x)^1$ for large $x < 1$, while becoming $(1-x)^2$ at the end point in agreement with the UV behavior of 1-gluon exchange binding.

Acknowledgments: KB acknowledges several beneficial conversations with Shi Chao, along with support from the graduate student visitor program of Argonne National Laboratory, which enabled several beneficial visits. This work was supported by the U.S. Department of Energy, Office of Science, Office of Nuclear Physics, contract no. DE-AC02-06CH11357; by the National Science Foundation, grant no. NSF-PHY1516138; and the Laboratory Directed Research and Development (LDRD) funding from Argonne National Laboratory, project no. 2016-098-N0 and project no. 2017-058-N0.

-
- [1] H.-W. Lin *et al.*, *Prog. Part. Nucl. Phys.* **100**, 107 (2018), [arXiv:1711.07916 \[hep-ph\]](#).
- [2] M. Deka *et al.*, *Phys. Rev.* **D91**, 014505 (2015), [arXiv:1312.4816 \[hep-lat\]](#).
- [3] Y.-B. Yang, R. S. Sufian, A. Alexandru, T. Draper, M. J. Glatzmaier, K.-F. Liu, and Y. Zhao, *Phys. Rev. Lett.* **118**, 102001 (2017), [arXiv:1609.05937 \[hep-ph\]](#).
- [4] P. C. Barry, N. Sato, W. Melnitchouk, and C.-R. Ji, *Phys. Rev. Lett.* **121**, 152001 (2018), [arXiv:1804.01965 \[hep-ph\]](#).
- [5] X. Ji, *Phys.Rev.Lett.* **110**, 262002 (2013), [arXiv:1305.1539 \[hep-ph\]](#).
- [6] H.-W. Lin, J.-W. Chen, S. D. Cohen, and X. Ji, *Phys. Rev.* **D91**, 054510 (2015), [arXiv:1402.1462 \[hep-ph\]](#).
- [7] C. Alexandrou, K. Cichy, V. Drach, E. Garcia-Ramos, K. Hadjiyiannakou, K. Jansen, F. Steffens, and C. Wiese, *Phys. Rev.* **D92**, 014502 (2015), [arXiv:1504.07455 \[hep-lat\]](#).
- [8] A. V. Radyushkin, *Phys. Rev.* **D96**, 034025 (2017), [arXiv:1705.01488 \[hep-ph\]](#).
- [9] M. Aicher, A. Schafer, and W. Vogelsang, *Phys. Rev. Lett.* **105**, 252003 (2010), [arXiv:1009.2481 \[hep-ph\]](#).
- [10] Z. F. Ezawa, *Nuovo Cim.* **A23**, 271 (1974).
- [11] G. R. Farrar and D. R. Jackson, *Phys. Rev. Lett.* **35**, 1416 (1975).
- [12] E. L. Berger and S. J. Brodsky, *Phys. Rev. Lett.* **42**, 940 (1979).
- [13] M. B. Hecht, C. D. Roberts, and S. M. Schmidt, *Phys. Rev.* **C63**, 025213 (2001), [nucl-th/0008049](#).
- [14] T. Nguyen, A. Bashir, C. D. Roberts, and P. C. Tandy, *Phys. Rev.* **C83**, 062201 (2011), [arXiv:nucl-th/1102.2448 \[nucl-th\]](#).
- [15] L. Chang, C. Mezrag, H. Moutarde, C. D. Roberts, J. Rodríguez-Quintero, *et al.*, *Phys.Lett.* **B737**, 23 (2014), [arXiv:1406.5450 \[nucl-th\]](#).
- [16] A. Bashir, L. Chang, I. C. Cloët, B. El-Bennich, Y.-X. Liu, *et al.*, *Commun.Theor.Phys.* **58**, 79 (2012), [arXiv:1201.3366 \[nucl-th\]](#).
- [17] I. C. Cloët and C. D. Roberts, *Prog. Part. Nucl. Phys.* **77**, 1 (2014), [arXiv:1310.2651 \[nucl-th\]](#).
- [18] P. C. Tandy, *Few Body Syst.* **55**, 357 (2014), [arXiv:1407.0494 \[hep-ph\]](#).
- [19] T. Horn and C. D. Roberts, *J. Phys.* **G43**, 073001 (2016), [arXiv:1602.04016 \[nucl-th\]](#).
- [20] K. D. Bednar, I. C. Cloët, and P. C. Tandy, *Phys. Lett.* **B782**, 675 (2018), [arXiv:1803.03656 \[nucl-th\]](#).
- [21] L. Chang and A. W. Thomas, *Phys. Lett.* **B749**, 547 (2015), [arXiv:1410.8250 \[nucl-th\]](#).
- [22] C. Chen, L. Chang, C. D. Roberts, S. Wan, and H.-S. Zong, *Phys. Rev.* **D93**, 074021 (2016), [arXiv:1602.01502 \[nucl-th\]](#).
- [23] C. Shi, C. Mezrag, and H.-s. Zong, (2018), [arXiv:1806.10232 \[nucl-th\]](#).
- [24] R. L. Jaffe, *Nucl. Phys.* **B229**, 205 (1983).
- [25] R. K. Ellis, W. J. Stirling, and B. R. Webber, *Camb. Monogr. Part. Phys. Nucl. Phys. Cosmol.* **8**, 1 (1996).
- [26] R. L. Jaffe, in *The spin structure of the nucleon. Proceedings, International School of Nucleon Structure, 1st Course, Erice, Italy, August 3-10, 1995* (1996) pp. 42–129, [arXiv:hep-ph/9602236 \[hep-ph\]](#).
- [27] M. Diehl, *Phys. Rept.* **388**, 41 (2003), [arXiv:hep-ph/0307382 \[hep-ph\]](#).
- [28] M. V. Polyakov and C. Weiss, *Dynamics of strong interactions. Proceedings, 37th Cracow School of Theoretical Physics, Zakopane, Poland, May 30-June 10, 1997*, *Acta Phys. Polon.* **B28**, 2751 (1997), [arXiv:hep-ph/9709436 \[hep-ph\]](#).
- [29] W. Bentz, T. Hama, T. Matsuki, and K. Yazaki, *Nucl. Phys.* **A651**, 143 (1999), [arXiv:hep-ph/9901377](#).
- [30] S.-x. Qin, L. Chang, Y.-x. Liu, C. D. Roberts, and D. J. Wilson, *Phys.Rev.* **C84**, 042202 (2011), [arXiv:1108.0603 \[nucl-th\]](#).
- [31] P. Maris and C. D. Roberts, *Phys. Rev.* **C56**, 3369 (1997), [nucl-th/9708029](#).
- [32] P. Maris and P. C. Tandy, *Phys. Rev.* **C62**, 055204 (2000), [nucl-th/0005015](#).
- [33] D. Brommel *et al.* (QCDSF-UKQCD), *Proceedings, 25th International Symposium on Lattice field theory (Lattice 2007): Regensburg, Germany, July 30-August 4, 2007*, *PoS LATTICE2007*, 140 (2007).
- [34] V. Bertone, S. Carrazza, and J. Rojo, *Comput. Phys. Commun.* **185**, 1647 (2014), [arXiv:1310.1394 \[hep-ph\]](#).
- [35] A. Buckley, J. Ferrando, S. Lloyd, K. Nordström, B. Page, M. Rüfenacht, M. Schönherr, and G. Watt, *Eur. Phys. J.* **C75**, 132 (2015), [arXiv:1412.7420 \[hep-ph\]](#).
- [36] J. S. Conway *et al.*, *Phys. Rev.* **D39**, 92 (1989).
- [37] J. Badier *et al.* (Saclay-CERN-College de France-Ecole Poly-Orsay), *Phys. Lett.* **B93**, 354 (1980).
- [38] C. Shi, L. Chang, C. D. Roberts, S. M. Schmidt, P. C. Tandy, and H.-S. Zong, *Phys. Lett.* **B738**, 512 (2014), [arXiv:1406.3353 \[nucl-th\]](#).